High Temperature Oxidation Issues in Fossil Boilers

Bruce A. Pint
Oak Ridge National Laboratory, P.O. Box 2008, Oak Ridge, TN 37831-6156
E-mail: pintba@ornl.gov; Telephone: (865) 576-2897; Fax: (865) 241-0215

Michael A. Bestor
Oak Ridge National Laboratory, P.O. Box 2008, Oak Ridge, TN 37831-6156
E-mail: bestorma@ornl.gov; Telephone: (865) 574-4451; Fax: (865) 241-0215

Sebastien Dryepondt
Oak Ridge National Laboratory, P.O. Box 2008, Oak Ridge, TN 37831-6156
E-mail: dryepondts@ornl.gov; Telephone: (865) 574-4452; Fax: (865) 241-0215

Ying Zhang
Dept. of Mechanical Eng, Tennessee Technological Univ., P.O.Box 5014, Cookeville, TN 38505-0001
E-mail: yzhang@tntech.edu; Telephone: (931) 372-3265; Fax: (931) 372-6340

ABSTRACT

This report covers the conclusion of a multi-year project that examined the oxidation resistance of Al-rich coatings and a new project examining the effect of higher CO_2 contents on corrosion mechanisms in oxy-fired coal-fueled boilers. The coating work primarily examined diffusion coatings for the steam side of typical ferritic (9-12%Cr) and austenitic (e.g., Type 304L) tube materials in accelerated testing at 650°-800°C in wet air. The final phase of this work has attempted to obtain additional coating failures to determine a critical Al content (at coating failure) as a function of exposure temperature. However, no failures have been observed for austenitic substrates including >25 kh at 700°C and >6 kh at 800°C. Preliminary results are presented from the oxy-firing project, where the initial focus is on ferritic alloys. Initial coal-ash experiments were conducted at 600°C to evaluate some of the test parameters and three different levels of CO_2 were investigated. An in-situ creep rig is being constructed to evaluate the effect of environment on creep properties. Initial ex-situ creep experiments are presented as a baseline.

INTRODUCTION

Coal-fired boilers include two aggressive corrosion environments, steam- and fire-side. A multi-year program was completed that explored the potential benefit for Al-rich coatings to protect Fe-base ferritic and austenitic alloys on the steam side where they form thick Fe-rich oxides. These oxides are thermal barriers on this heat transfer surface and steam-side scale spallation potentially leads to (1) erosion in the steam turbine from ferritics and (2) catastrophic tube failures in austenitic tubes.[1] The use of Al alloy additions or Al-rich coatings to improve oxidation resistance has been studied for many years.[2-7] The goal of this project was to identify the potential benefits and barriers associated with the use of Al-rich coatings on ferritic-martensitic (FM) and Fe-base austenitic alloys for high temperature and pressure conditions such as the DOE Advanced Ultra-Supercritical (A-USC) steam program to improve the efficiency of coal-fired boilers.[8] Factors such as thermal expansion, interdiffusion and mechanical integrity have been investigated using model coatings on representative Fe-base alloys.[9-15] Some final results are presented on the laboratory studies conducted at 650°-800°C on model coatings made by chemical vapor deposition (CVD) and pack cementation processes. These experiments were conducted to improve the lifetime model that was developed based on the long-term oxidation and interdiffusion studies.[12] Lifetimes for aluminized austenitic substrates are significantly longer than those for ferritic substrates.

The new project begun in 2010 is intended to explore a broader array of corrosion issues in coal-fired boilers, including the effect of oxy-firing conditions on fireside corrosion mechanisms. Replacing air with oxygen in coal-fired boilers and concentrating the CO_2 by using flue-gas recirculation also may increase the H_2O and SO_2 contents in the flue gas.[16] It is anticipated that the change in gas composition will increase the fireside corrosion rate. The goal of this work is to better understand the corrosion mechanisms responsible for this increase, with and without ash deposits. In addition to fireside corrosion, this project also will examine the effect of higher steam temperatures on current and advanced alloys. In addition to oxidation testing, the effect of steam oxidation on creep performance also will be investigated using in-situ creep testing in steam. Some initial results are presented on the effect of higher CO_2 levels on fireside corrosion in synthetic coal ash on a range of commercial and model alloys with the current focus on ferritic steels at 600°C. Current ex-situ creep results of Ni-base alloys are also presented.

EXPERIMENTAL PROCEDURE

A range of Fe-base alloy substrates (~18 x 12 x ~1.5 mm) was coated with the focus on commercial Grade 91 (Fe-9.3 at.%Cr-0.6Mo-0.5Mn-0.3V-0.55Si-0.2Ni-0.5C-0.22N-0.005S) and austenitic type 304L stainless steel (Fe-19.7 at%Cr-7.9Ni-1.8Mn-0.15Mo-0.76Si-0.32N-0.09C-0.006S). Details on the laboratory-scale CVD reactor and coating conditions are described elsewhere.[14] Coated specimens were cleaned in acetone and methanol prior to exposure and exposed with the as-coated surface finish. Specimen mass changes (±0.02 mg/cm^2 accuracy) were measured using a Mettler Toledo model AG245 balance. Cyclic oxidation exposures were conducted with a 100h cycle time at temperature with specimens in an alumina boat with faces parallel to the gas stream. An environment of air + 10±1 vol.% water vapor was used to determine coating performance as this environment causes rapid oxidation of the uncoated substrates,[9,10,13] similar to a steam environment. The fireside corrosion experiments were conducted with rod specimens (6mm diameter x ~25mm long) in a porous alumina crucible with a synthetic ash of 30%Fe_2O_3-30%Al_2O_3-30%SiO_2-5%Na_2SO_4-5%K_2SO_4. The alloys included Grade 22 (Fe-2.4Cr-0.5Mo), Grade 315 (Fe-3.2Cr-0.5W-0.4Mo), Grade 91, Save12 (Fe-10.4Cr-2.5Co-0.9W), Save25 (Fe-19Ni-24Cr-3Cu-0.3W), 310HCbN (Fe-19Ni-27Cr-1.2Mn), CCA617 (Ni-24Cr-11Co-5Mo-3Al) and IN740 (Ni-25Cr-19Co-2Fe-2Al-2Ti-1Nb). The exposure was at 600°C for 500h with a base gas of N_2-15%CO_2-3.5%O_2-0.25%SO_2, which was mixed with CO_2 to vary the gas composition. After exposure, the ash was removed before weighing. For characterization, specimens were examined by field emission gun, scanning electron microscopy (SEM) equipped with energy dispersive x-ray analysis (EDXA), standard metallographic sectioning, and by electron probe microanalysis (EPMA) using wavelength dispersive x-ray analysis.

RESULTS AND DISCUSSION

COATING RESULTS

Figure 1 shows mass gain data at 700° and 800°C. These temperatures were selected to accelerate the time to coating failure. Uncoated Fe-base alloys show rapid oxidation rates in this environment due to the formation of Fe-rich oxide nodules. When the coating can no longer form a protective Al-rich oxide, Fe-rich oxide nodules form and the mass gain rapidly increases. The 700°C results include the ~250µm thick coatings on 304L and Gr.91 that were stopped after a 20kh exposure without oxide nodule formation.[17] Of more interest are the ~50µm "thin" coatings on FM steel and 304L substrates. In addition to the Gr91 failure reported earlier, a failure was observed for a coated Gr.122 (Fe-11.4at.%Cr-0.6%W) specimen at ~5 kh and a second coated specimen was stopped after 8kh for analysis. A coated Gr.92 (Fe-9.9at.%Cr-0.6%W) specimen has completed ~12 kh and showed a mass increase around 8kh, but not as large a jump

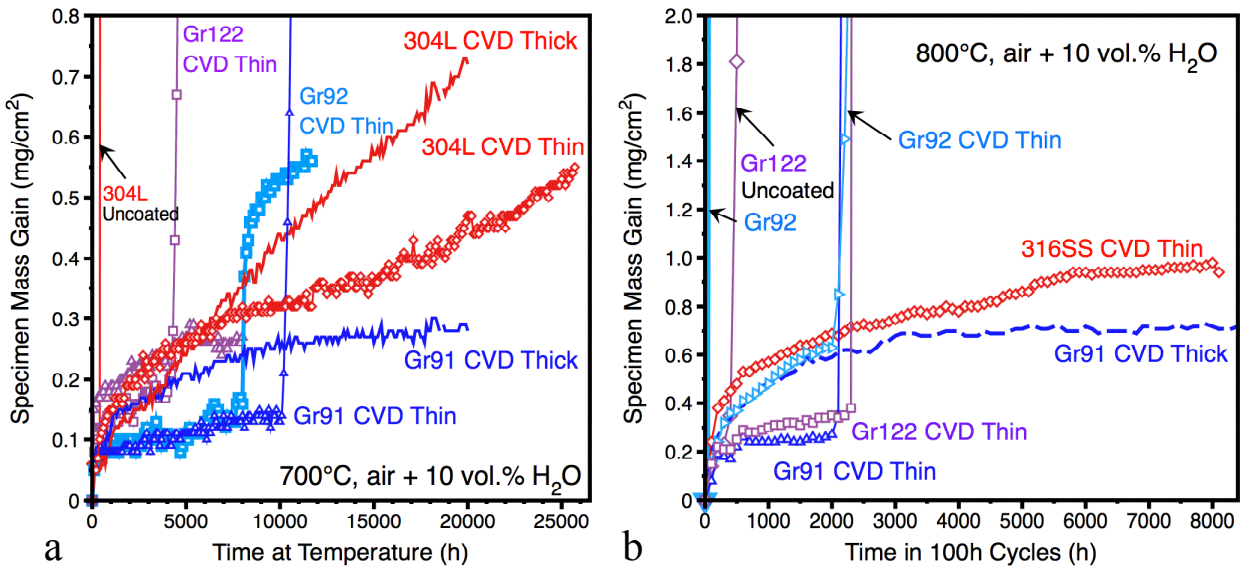

Figure 1. Specimen mass changes during 100h cycles in wet (10 vol.%H_2O) air for uncoated and thin (~50µm) and thick (~250µm) CVD coatings on Fe-base substrates at (a) 700°C and (b) 800°C.

as the other failed specimens. In contrast, the 304L specimen with a ~50µm thick coating has passed 26kh with a relatively low mass gain. This shows at least a 2X increase in lifetime for the austenitic substrate compared to the coated FM specimens. Likewise at 800°C, all of the FM substrates failed after <2.5kh but the coated type 316 (Fe-19.9at%Cr-8.9Ni-1.7Mn-1.4Mo-1.9Si) stainless steel specimen has exceeded 8kh without failure. The mass gain for this specimen is close to that for the 250µm coating on Gr.91 that was stopped after 20kh at 800°C (dashed line in Figure 1b).

The failed FM specimens were sectioned and the remaining Al content was measured in areas where the coating had not failed.[13,15,17] Examples are given in Figure 2a. The Gr.122 specimen at 650°C was inadvertently exposed at ~900°C for 4h due to a furnace malfunction. After this excursion, the mass gain increased and the specimen was stopped and sectioned. The surface Al content in these failed specimens defines the critical Al content at coating failure, C_b, which is the failure criteria needed to model coating lifetime, Figure 2b.[12] The current results in wet air suggest that C_b decreases with increasing temperature. The value for the 650°C specimen (with the 900°C excursion) is similar to the lowest level observed by Agüero[7] after steam testing at 650°C for 60kh. One failed Gr.91 specimen exposed at 800°C in 17bar steam[18] also is shown in Figure 2b. This coating had a higher starting Al content due to a higher Al activity[19] but began to form oxide nodules after only 3kh (using 500h cycles). Further work is needed to determine if there is a different C_b value for exposures in steam compared to wet air.

By establishing a failure criteria as a function of temperature, it should be possible to model coating lifetime based on starting Al content and operating temperature. The framework of a model has been developed for FM steels[12] and further work is being conducted at Tennessee Technological University to improve the model. For austenitic steels, there has been less progress because no coatings have failed to establish a failure criteria. The inhibited interdiffusion due to the ferritic coating-austenitic substrate phase boundary will require more extensive modeling work.

A project to move these coating results towards commercialization has been funded by the Electric Power Research Institute (EPRI) and coatings are being made on austenitic steel substrates for further evaluation.

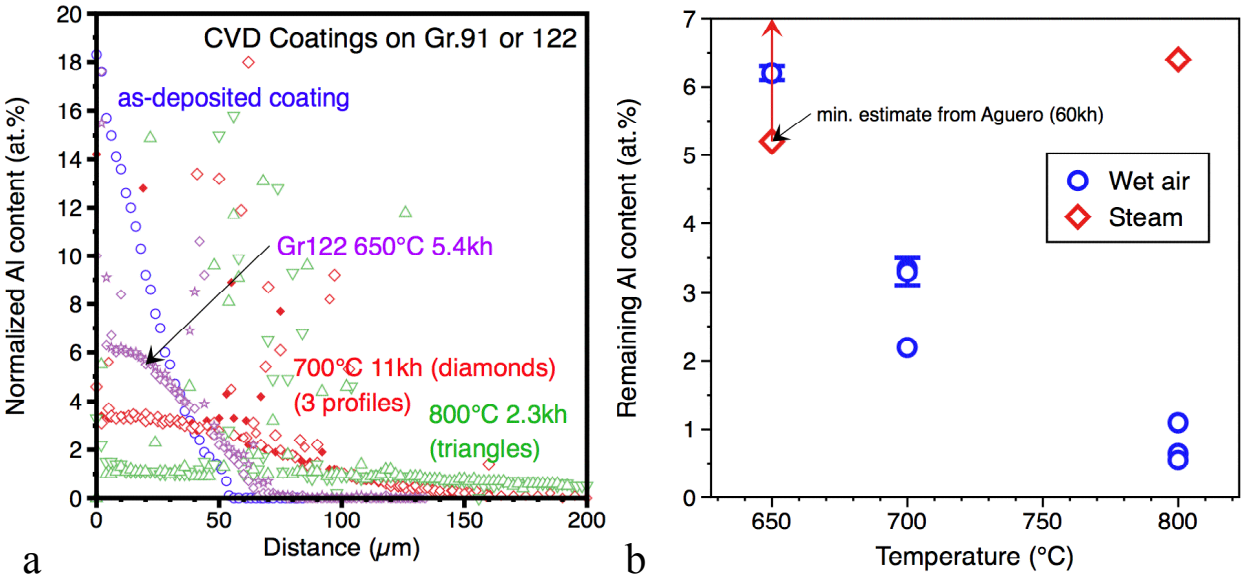

Figure 2. (a) EPMA Al line profiles for as-deposited and failed coatings and (b) summary of the surface Al content in failed specimens. Three of the data points in (b) were taken from profiles in (a).

EX-SITU CREEP RESULTS

A rig for measuring creep in the presence of steam (1bar) is currently under construction. Initial work to establish the creep conditions has been previously conducted on FM steels[11] and additional work was performed on Ni-base alloys of interest for the A-USC program. Rather than in-situ testing, these experiments were performed ex-situ by exposing 25mm long tensile specimens (2 x2mm gage) to 17 bar steam for 2 and 4 kh at 800°C and then performing creep testing at 800°C with a load of 140MPa, Figure 3. The first two alloys examined were 718 (Ni-20at.%Cr-18Fe-3Nb-2Mo-1Al-1Ti) and 230 (Ni-27Cr-4W). Alloy 718 had a lower creep rate as-received but showed a significant increase after exposure. Figures 3c and 3d show comparable oxide thickness and internal oxidation on these alloys.[18] However, alloy 718 typically operates at <700°C. Therefore, the increase in creep rate may be due to an alloy instability rather than an effect of the steam exposure. Additional work is needed to evaluate similar specimens with a 2 kh anneal in an inert environment. Specimens of alloys 740 and 617 also were exposed and will be creep tested ex-situ followed by in-situ testing. After several Fe- and Ni-base alloys are evaluated in the in-situ creep rig, a decision will be made about continuing this work.

FIRESIDE CORROSION RESULTS

In order to gain a better understanding of the test parameters, the initial fireside corrosion experiments exposed one set of rod specimens fully covered with ash (~9 g) and the second set only half covered with ash (~4 g) with the upper part of the rod exposed. The half-exposed procedure has been used to determine the effect of the gas mixture with and without ash in contact with a single specimen. Figure 4a shows the mass change results for the specimens after 500h at 600°C with the same N_2-CO_2-O_2-SO_2 gas mixture. Generally, the mass gains were higher after the full ash exposure, as expected. However, the mass change can be complicated by residual ash stuck to the specimen and spallation of the thick oxide. Overall, the stainless steels (310HCbN and Save25) showed the lowest mass gains, the Ni-base alloys were slightly higher and the low alloy and FM steels showed the most significant attack. In order to further understand the attack under these conditions, specimens were examined metallographically. Figures 4b and 4c show

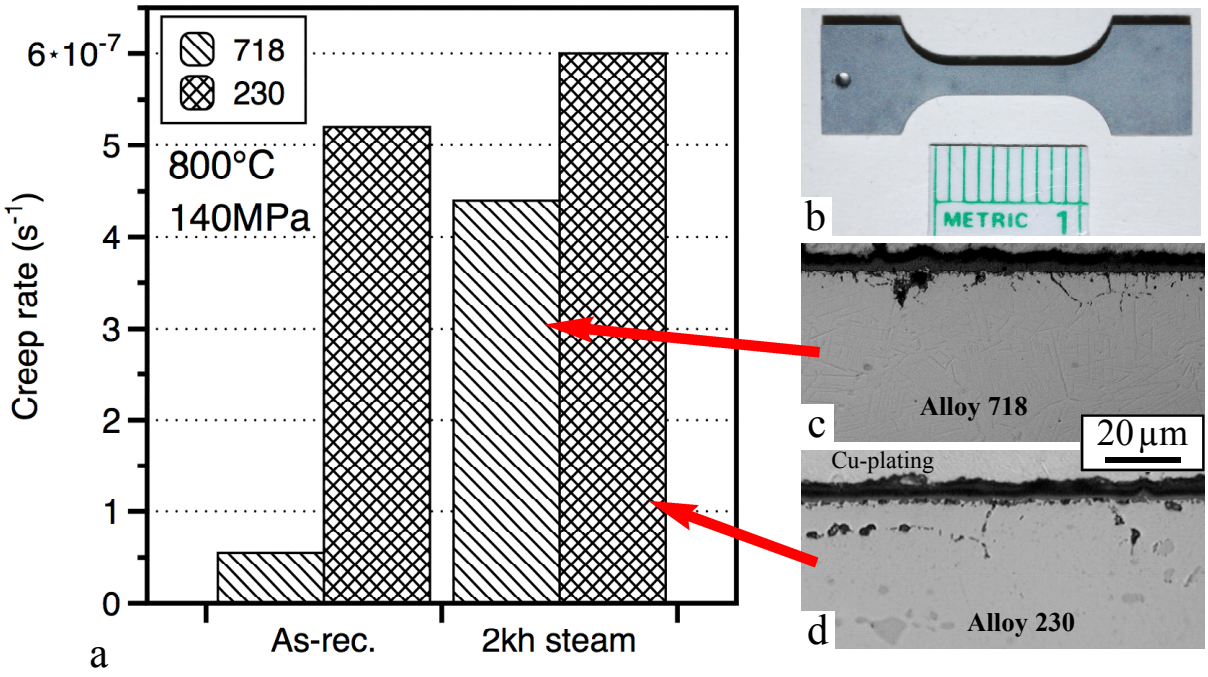

Figure 3. (a) Creep rate at 800°C for two Ni-base alloys with and without exposure for 2kh at 800°C in 17bar steam. Alloy 718 showed a greater difference than alloy 230. The creep specimen is shown in (b). Polished cross-sections of coupons with similar exposures are shown for (c) alloy 718 and (d) alloy 230.

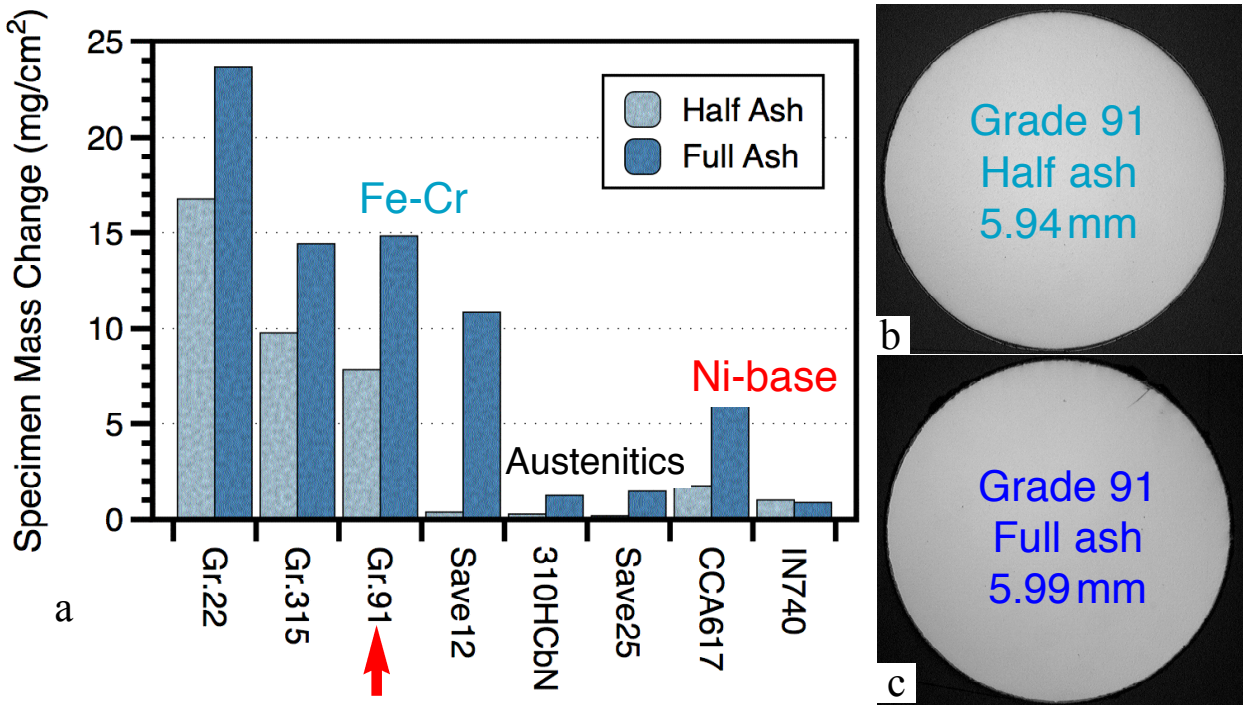

Figure 4. (a) Mass gain results for rod specimens exposed for 500h at 600°C in a fireside corrosion exposure either half-covered or fully covered with synthetic ash. Cross-sections of the Gr.91 specimens are shown in (b) and (c).

transverse sections through the Grade 91 rod specimens in both cases from the end of the specimen submerged in the synthetic ash. Measurements from the sections showed slightly different metal loss from the original 6mm diameter, with an average remaining diameter of 5.94mm after the half-ash experiment and 5.99mm after the full-ash exposure. There was no indication of significant internal penetration below the oxidation front in either case. To compare the ash-exposed end to the end above the ash, longitudinal sections also were made from these specimens. Figure 5 shows similar sections from both specimens. The end not exposed directly to ash is shown in Figure 5a. As might be expected, the oxide looks different than that formed on the full-ash covered specimen, Figure 5b. However, the oxide on the lower part of the half-ash covered specimen also appeared different than the lower part of the full-covered specimen, Figure 5c and 5d, respectively. These results suggest that ash-covered results may be affected depending on the extent the specimen was covered in ash, further complicating an already complicated experiment. A more sensible strategy appears to expose separate specimens with and without ash to determine the role of ash on the corrosion rate and mechanism.

Subsequent experiments were conducted with the specimens fully covered with ash. Figure 6a shows the mass gain data from the initial test shown in Figure 4a and two subsequent exposures where additional CO_2 was mixed with the base gas to create higher CO_2 levels in the experiment. In general, these results are in agreement with prior studies that suggested an increased corrosion rate due to higher CO_2 levels.[20,21] The materials retained a similar ranking with the austenitic steel showing the lowest mass gains in these environments, followed by the Ni-base alloys, the FM steels and the low-alloy Grade 22 steel with the highest mass gain. The scatter in the mass gain data in Figure 6a needs to be further investigated using metallography to quantify the attack. In addition to the commercial alloys, model alloys also were exposed to further understand the role of composition and provide guidance for alloy and coating development. For example, in Figure 6b the mass gain for two model binary alloys, Fe-15Cr and Fe-20Cr, are plotted with the other steels. Again, a more thorough understanding will be gained by metallographic sections of these specimens which will be presented in future reports as the project progresses.

In addition to focusing on metal loss and depth of penetration for additional characterization, future experiments will include water vapor to better simulate the combustion environment and the changes associated with oxy-firing. Depending on the type of flue gas recirculation, the oxy-fired environment

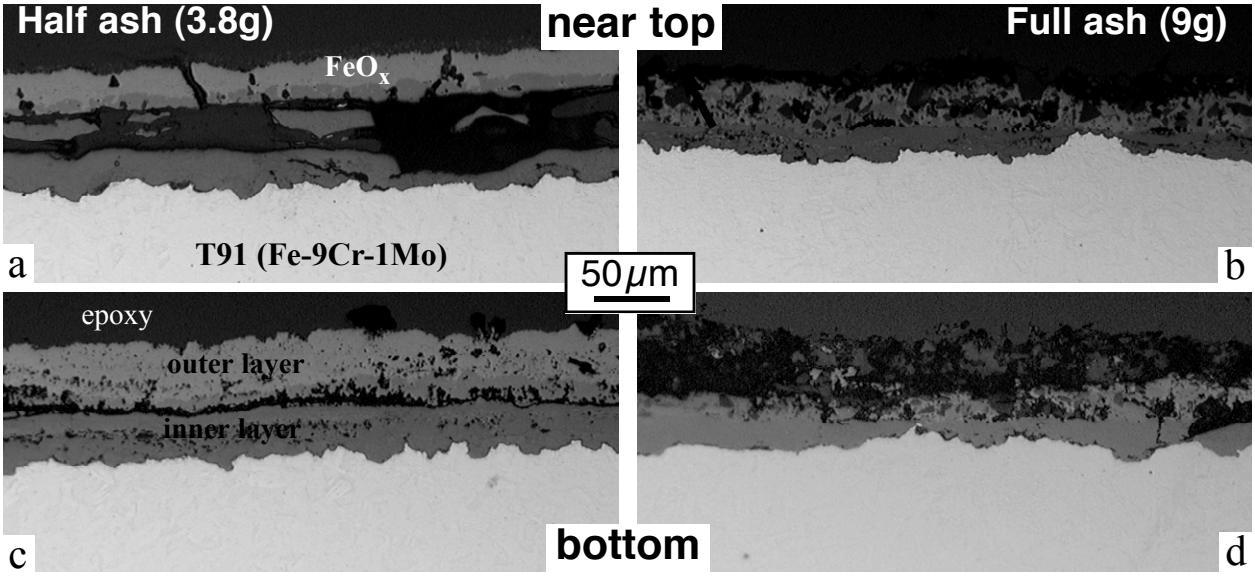

Figure 5. Light microscopy of polished sections of Grade 91 specimens with half-ash (a,c) and full-ash (b,d) fireside corrosion exposures for 500h at 600°C; (a,b) show sections near the top of the specimen and (c,d) near the bottom.

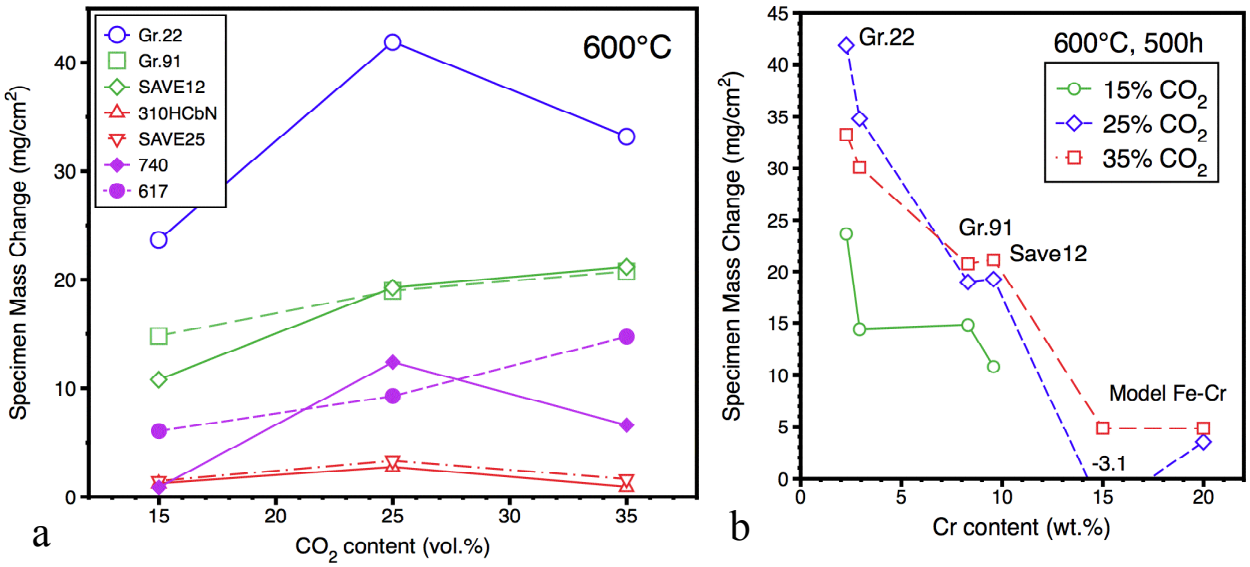

Figure 6. Mass gain results for rod specimens exposed for 500h at 600°C in a fireside corrosion exposure with full ash exposure: (a) as a function of CO_2 content in the gas and (b) as a function of Cr content in the Fe-base alloys.

could contain higher levels of H_2O and SO_2.[16] However, cooling or cleaning the flue gas could reduce those differences. Several environments will be evaluated to determine the role of each of these parameters on the rate of corrosion for a core group of alloys. In addition to the commercial alloys, more model alloys will be exposed, including model Fe-Cr-Ni alloys that may provide a less expensive weld overlay composition to protect boiler waterwalls and steam tubes.[22-24]

SUMMARY

Final results were presented from the conclusion of a multi-year project that examined the oxidation resistance of Al-rich coatings. The failure of additional coated ferritic-martensitic specimens has allowed the critical Al content to be determined as a function of exposure temperature from 650°-800°C and compared to other studies. This information has been used to develop a coating lifetime model[12] that is being further refined as more data becomes available. No failures have been observed for similar coatings on austenitic steel substrates exposed at 700° and 800°C for ~3X longer times than the ferritic substrates. The longer life is attributed to the ferritic coating-austenitic substrate inhibiting the Al interdiffusion for these substrates.[15] Additional work will be needed to develop a coating lifetime model for austenitic steels. The promising results for austenitic steels are being further pursued with an EPRI-funded project at ORNL with a commercial coating partner.

Preliminary results were presented from a new project examining the effect of oxy-firing conditions on fireside corrosion mechanisms in coal-fired boilers. Initial experiments at 600°C compared results when commercial specimens were fully covered with synthetic ash to those when the specimen was only half covered. Subsequent experiments increased the CO_2 composition in the experiment with full ash coverage to simulate the higher CO_2 contents expected with oxy-firing. Higher mass gains suggest an increase in the amount of attack with higher CO_2 contents. Also, initial ex-situ creep experiments were conducted as a baseline for future in-situ creep testing in the presence of steam. Two in-situ creep rigs are being constructed to determine the effect of steam on creep resistance.

ACKNOWLEDGMENTS

The author would like to thank L. Walker, T. Brummett, K. Cooley and H. Longmire for assistance with the experimental work. P. F. Tortorelli and J. A. Haynes provided helpful comments on the manuscript. The research was sponsored by the U.S. Department of Energy, Fossil Energy Advanced Research Materials Program (V. Cedro, project monitor).

REFERENCES

1. I. G. Wright, A.S. Sabau, and R. B. Dooley, *Mater. Sci. Forum*, 595-598 (2008) 387.
2. N. R. Lindblad, *Oxid. Met*., 1 (1969) 143.
3. N. V. Bangaru and R. C. Krutenat, *J. Vac. Sci. Tech. B*, 2 (1984) 806.
4. M. Zheng and R. A. Rapp, *Oxid. Met.*, 49 (1998) 19.
5. S. W. Banovic, J. N. Du Pont and A. R. Marder, *Mater. High Temp.*, 16 (1999) 195.
6. V. Rohr and M. Schütze, *Mater. Sci. Forum*, 461-464 (2004) 401.
7. A. Agüero, R. Muelas, M. Gutiérrez, R. Van Vulpen, S. Osgerby and J. P. Banks, *Surf. Coat. Tech.*, 201 (2007) 6253.
8. R. Viswanathan and W. Bakker, *J. Mater. Eng. Performance*, 10 (1) (2001) 81.
9. B. A. Pint, Y. Zhang, P. F. Tortorelli, J. A. Haynes and I. G. Wright, *Mater. High Temp.*, 18 (2001) 185.
10. Y. Zhang, B. A. Pint, G. W. Garner, K. M. Cooley and J. A. Haynes, *Surf. Coat. Tech*., 188-189 (2004) 35.
11. S. Dryepondt, Y. Zhang and B. A. Pint, *Surf. Coat.Tech.*, 201 (2006) 3880.
12. Y. Zhang, A. P. Liu and B. A. Pint, *Mater. Corr.*, 58 (2007) 751.
13. B. A. Pint, Y. Zhang, L. R. Walker and I. G. Wright, *Surf. Coat.Tech.*, 202 (2007) 637.
14. Y. Zhang, B. A. Pint, K. M. Cooley and J. A. Haynes, *Surf. Coat. Tech.*, 202 (2008) 3839.
15. B. A. Pint and Y. Zhang, *Mater. Corr.*, in press.
16. B. Bordenet and F. Kluger, *Mater. Sci. Forum*, 595-598 (2008) 261.
17. B. A. Pint, Y. Zhang, L. R. Walker and I. G. Wright, Proc. 22nd Annual Conf. Fossil Energy Materials, U.S. Dept. of Energy (2008).
18. I. G. Wright and R. B. Dooley, *Int. Mater. Rev*., 55 (3) (2010) 129.
19. B. A. Pint, *J. Nucl. Mater.*, in press.
20. S. Sroda, M. Makipaa, S. Cha and M. Spiegel, *Mater. Corr.*, 57 (2006) 176.
21. B. S. Covino, Jr., S. A. Matthes, and S. J. Bullard, "Effect of Oxyfuel Combustion on Superheater Corrosion," NACE Paper 08-456, Houston, TX, presented at NACE Corrosion 2008, New Orleans, LA, March 2008.
22. D. B. Meadowcroft, *Mater. Sci. Eng.*, 88 (1987) 313.
23. T. Heston, *Welding Journal*, 79(7) (2000) 45.
24. L. Paul, G. Clark, A. Ossenberg-Engels, *Power Eng.*, 111 (9) (2007) 64-68.